Digest Journal of Nanomaterials and Biostructures Vol. 15, No. 4, October-December 2020, p. 1189- 1195

CHARACTERIZATION OF SILVER CONTENT UPON PROPERTIES OF NANOSTRUCTURED NICKEL OXIDE THIN FILMS

H. T. SALLOOM[a], E. H. HADI[b], N. F. HABUBI[b], S. S. CHIAD[b], M. JADAN[c], J. S. ADDASI[d,*]

[a]*Al-Nahrain Nanorenewable Energy Research Centre, Al-Nahrain University, Baghdad, Iraq*

[b]*Department of Physics, College of Education, Mustansiriyah University, Baghdad, Iraq*

[c]*Department of Physics, College of Science, Imam Abdulrahman Bin Faisal University, P.O. Box 1982, 31441 Dammam, Saudi Arabia*

[d]*Department of Applied Physics, College of Science, Tafila Technical University, 66110 Tafila, Jordan*

The influence of two silver contents (2% and 4%) on NiO films were studied in terms of structural and optical properties. Ag doped NiO films were grown on glass and n-type silicon substrates heated at 400°C by chemical pyrolysis method. Optical transmission measurements showed up to 60% transparency in the visible area for undoped NiO and decreased with increasing Ag content. X-ray diffraction assures the existence of epitaxial growth with the c-axis. Average particle size, surface roughness and energy gap were decreased also. Rectifying characteristics of junctions deposited films on n-type silicon has been analyzed. Transparent conductive films showed excellent properties to be adopted for solar cells and optical sensors.

(Received July 24, 2020; Accepted November 27, 2020)

Keywords: Silver-doped nickel oxide, Optical properties, X-ray diffraction, Photovoltaic, Thin films

1. Introduction

Over the years, nanostructure metal oxide films have gained much interest due to their broad application including radiation detectors, gas sensors, optoelectronic devices, solar cells, laser materials, and thermoelectric devices, [1-3]. NiO is a metal oxide with semi-transparent, p-type semiconducting material and large bandgap width of almost 3.8eV facilitates its option as light detectors and solar cells [4]. Also, NiO shows attractive electric, electro-chromic and thermoelectric properties [5-7]. To explore the new applications, various studies have been conducted when the doping of ions into NiO lattice modifies these properties using many different chemical and physical approaches. In this regard, Nandy et al. [8] studied the doping of Aluminum atoms into NiO film to enhance p-type conductivity. Boutwell et al. [9] prepared magnesium NiO:Mg thin films by a sol–gel and spin coating methods to enhance the optical transmission in UV–visible region. Kate et al. [10] addressed the effect of Co doping on structural, optical and compositional properties of NiO thin films. However, few reports have examined silver NiO:Ag as silver has a well-known surface plasmon resonance (SPR) to modulate the optical response of Ag-doped films. For example, Nagamuthu et al. [11] synthesized NiO:Ag honeycomb nanoarrays via a surfactant-assisted hydrothermal for supercapacitor applications. Ying Wei et al. [12] demonstrated NiO:Ag as inorganic hole transporting layer for perovskite solar cells (PSCs). Zheng et al. [13] considered the effect of Ag-doping on transmittance and surface topography of NiO films, they showed that NiO: Ag by a simple solution process is a promising material for high achievement inverted PSCs appropriate for tandem solar cells. Nevertheless, the above requirements should be ensured via a suitable fabrication method.

* Corresponding author: addasijihad@gmail.com

In this contribution, pure, 2% and 4% Ag doped NiO was prepared using a low cost chemical pyrolysis technique. Structural properties, absorption and transmittance of the prepared nickel oxide films are examined. The influence of silver doping on optical energy gap and rectifying behavior is also shown.

2. Experimental work

Thin films of NiO doped by Ag were prepared using chemical spray pyrolysis (CSP) method. The aqueous solution containing 1 M of NiO acetate ($NiCl_2.6H_2O$) and deionized water was used to get the matrix solution. To prepare doping material, $AgNO_3$ was used to obtain volumetric percentage of 2% and 4% that was added to the matrix, Substrate temperature was preserved at 400 ^oC through preparing process. Cleaning procedure and optimization of deposition parameters have been mentioned in our previous work [14, 15]. Thickness of the films was found gravimetrically to be about 350 ± 30 nm, then optical measurements were recorded using UV-Visible spectrophotometer (Model: Shimadzu Japan) double beam spectrophotometer. Structural properties were determined by X-ray diffractometer (Model: XRD-6000 Shimadzu, Japan). Surface topography was checked by AFM (model: AA 3000 Scanning Probe Microscope).

3. Results and discussion

Fig. 1 displays XRD patterns of pristine and Ag doped NiO thin films grown by spray pyrolysis method. The figure offers a diffraction peak at (2θ=37.1 °) with Miller indices (111) indicating a cubic crystal structure, which agreed with ICDD card No-73-1523. By increasing Ag concentration, there is a slight shift in the position 2θ towards the lower from 37.1 for undoped film to 36.7 for 4% Ag:NiO films and this could be assigned to the replacement of Ni ions by Ag ions. Crystalline size (D) was calculated from the highest intensity peaks utilizing Scherrer's equation [14-16].

$$D = \frac{0.9\lambda}{\beta cos\theta} \quad (1)$$

where λ is the wavelength of the X-rays used (1.5406 Å), β and θ are full width at half maximum (FWHM) and the diffraction angle respectively. The crystalline size has been found to vary from 15 to 31 nm with Ag concentration as listed in Table 1.

Other structural parameters such as dislocation density (δ) and strain (ε) are also evaluated. δ gives number of defects in the films [17-19], the values of (δ) and (ε) listed in Table 1 shows the structural parameters estimated from

$$\delta = \frac{1}{D^2} \quad (2)$$

$$\varepsilon = \frac{\beta cos\theta}{4} \quad (3)$$

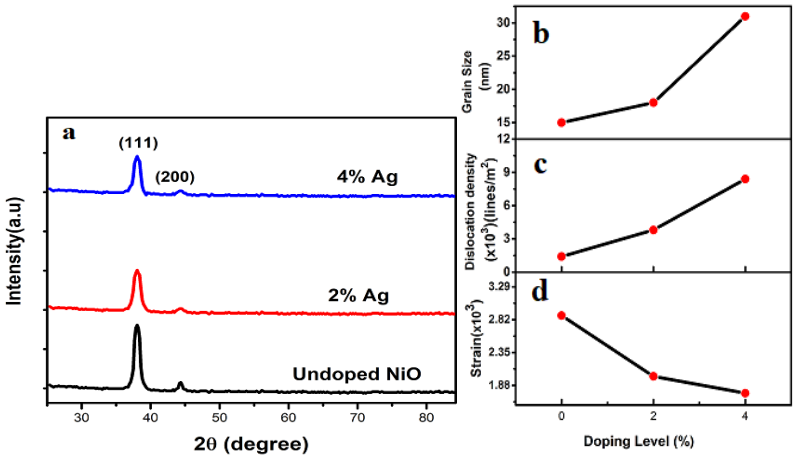

Fig. 1. XRD-patterns (a) crystalline size (b) Dislocation (c) Strain (d) of the prepared films.

Table 1. Grain size, optical band gap and structural parameters of the prepared films.

Sample	Grain size (nm)	Optical bandgap (eV)	Dislocations density ($\times10^{14}$) (lines/m^2)	Strain ($\times10^{-3}$)
NiO pure	15	3.82	1.4	2.88
NiO: 2% Ag	18	3.67	3.8	2.01
NiO: 4% Ag	31	3.55	8.4	1.77

Atomic force microscope AFM micrographs and their roughness analysis of prepared NiO:Ag films are demonstrated in Fig. 2 a-i. The 3-D images and grain size distribution are given in Fig. 2 a-f, they exhibit spherical nano-grains ranged from 97.78 nm for pure NiO to 76.32 nm for 4% Ag doped NiO. The change in surface morphology ranged from 16.8 to 5.6 nm with the increase of silver doping. By increasing Ag doping, the decrease in average surface roughness was due to the reduction in grain size. The reduction values agree with crystallite size variation established from XRD data. Same trend in roughness values for NiO:Ag and NiO:Co are reported by Zheng et al. 2018 [13], Taşköprü et al. (2015) [11] respectively. The influence of Ag doping on AFM parameters namely grain size (D), surface roughness (R_a) and root root-mean-square (R_{rms}) are shown in Fig. 2 g, h and i respectively. Table 2 represents the values of AFM parameters.

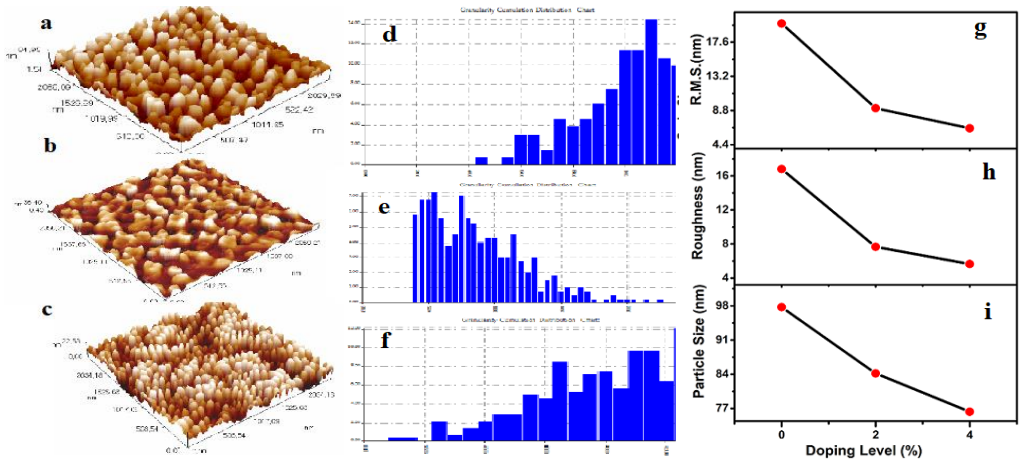

Fig. 2. AFM images of the prepared films (a, b and c), granularly distributed (d, e and f) and variation of AFM parameters via doping (g, h and i).

Table 2. AFM parameters of the deposited films.

Sample	D (nm)	R_a (nm)	R_{rms} (nm)
NiO pure	97.78	16.8	20
NiO: 2%Ag	84.17	7.6	9.1
NiO: 4%Ag	76.32	5.6	6.5

Optical transmittance and absorbance measurements of prepared films were performed at spectral region (300 to 900) nm and room temperature. Results are shown in Fig. 3, 4. where all films were transparent in that region. Pure NiO films showed up to 60 % optical transmission and then considerably decreased with the increase of Ag doping level. These results were in accord with Ag-doped NiO films deposited via spin coating [13] and sputtering [20] methods. The absorption edge is shifted to higher wavelengths according to the increase in silver content as shown in Fig. 3 a, this can be due to the presence of inter-band transitions at localized states in the energy gap.

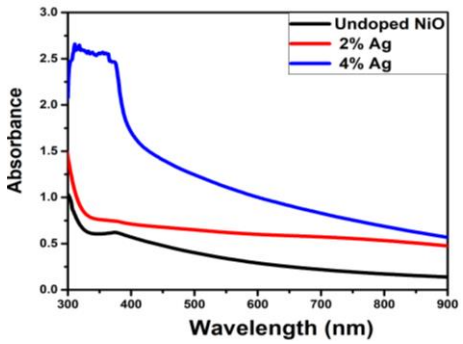

Fig. 3. Absorbance against wavelength for the grown films.

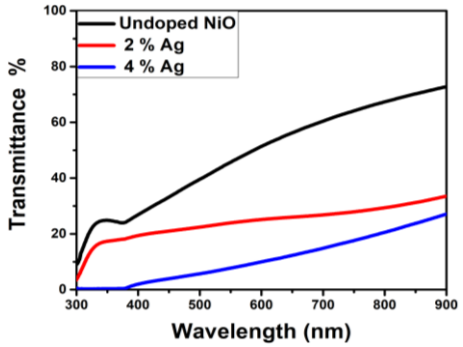

Fig. 4. Transmittance for the prepared films.

By using Tauc's relation, optical energy gap of pristine and Ag doped NiO were found from [21-25]:

$$\alpha h\upsilon = G(h\upsilon - E_g)^2 \tag{4}$$

where α, $h\upsilon$, G and E_g are absorption coefficient, photon energy, proportional constant and energy gap respectively. By using of x-axis intersection of αhν versus hν plots, the optical energy gap was determined as shown in Fig. 5. Eg. values decreased from 3.82 to 3.55 eV with increasing of Ag doping level.

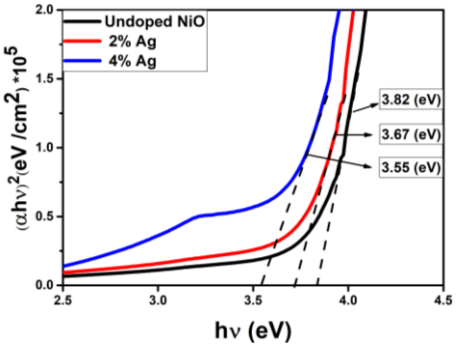

Fig. 5. $(\alpha h\nu)^2$ versus hv of the prepared thin films.

Fig. 6 displays the I-V characteristics of pure NiO and NiO:Ag deposited on n-Si by CSP method. Reverse to forward bias currents beneath dark and illumination have measured at –5 V to +5 V. Ideality factor n and barrier height Φ_b has been determined utilizing thermionic emission (TE) equation. From Fig. 6, it can be noticed that pure and Ag doped-NiO/n-Si diodes exhibit not only significant rectifying properties in dark but also good light response under illumination, current densities (J) and diode parameters (n, Φ_b) were calculated as follows [26-29]:

$$J = J_0 \exp\left(\frac{qV}{nKT} - 1\right) \quad (5)$$

$$n = \frac{q}{KT}\frac{dV}{d(\ln J)} \quad (6)$$

$$\phi_b = \frac{KT}{q}\ln\left(\frac{AA^*T^2}{J_0}\right) \quad (7)$$

where A, A^* and J_o are active area, Richardson constant and saturated current density respectively. From Eq. 5, n and J_o values were calculated for (V > 3kT/q).

As listed in Table 3, rectifying parameters n and Φ_b values under darkness were varied from (4.6 - 4.8) and (0.81 - 0.86) eV. These values have changed to (4.1 - 4.3) and (0.80 - 0.82) eV for measurements under 100 mW light intensity. Although n values were higher than unity (optimum rectifying), the data suggest non-ideal action of fabricated p-NiO/nSi junctions [30, 31]. Moreover there is a considerable enhancement in reverse current values with increasing Ag content and this could be due to increase in carrier concentrations. This behavior agrees with the findings reported by Ibrahim et al [32] related to lutetium oxide (Lu_2O_3 doped –NiO) thin films and Karatas et al [33] related to Ru doped ZnO/p- Si junction diodes.

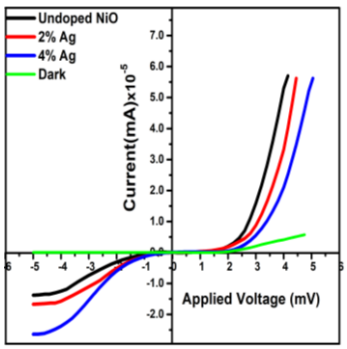

Fig. 6. The I-V plots of the fabricated NiO/ Silicon junctions.

Table 3. Rectifying parameters of the pure NiO/n-Si, 2% AgNiO/n-Si and 4% AgNiO/n-Si diodes under dark and illumination conditions.

Diode	Dark		illumination	
	Φ_b (eV)	n	Φ_b (eV)	n
NiO/n-Si	0.86	4.6	0.82	4.1
NiO: 2% Ag / n-Si	0.82	4.75	0.81	4.2
NiO: 4% Ag / n-Si	0.81	4.8	0.80	4.3

4. Conclusions

In summary, pure and silver doped NiO films were fabricated successfully via chemical pyrolysis technique. The influences of two silver concentrations (2% and 4%) on optical, morphological structural and electrical characteristics have been examined. XRD result displayed the NiO cubic structure, the tuning of optical bandgap was predicted by UV-V spectrum analysis. Minimum bandgap value of 3.55 eV was attained for 4% Ag doped NiO films. Rectifying characteristics for pure and Ag doped p-type NiO/n-type Silicon junction diode were calculated in dark and under illumination. This photo-response behavior makes these diodes suitable as detection devices.

Acknowledgments

Authors would appreciate Mustasiryah University and Al-Nahrain University for their support.

References

[1] S. A. Aslanzadeh, Chin. J. Phys. **56**, 1917 (2018).
[2] S. R. Atchuta, S. Sakthivel, H. C. Barshili, Sol. Energy Mater. Sol. Cells **200**, 109917 (2019).
[3] R. Deng, B. Yao, Y. F. Li, Y. Xu, J. C. Li, B. H. Li et al., J. Lumin. **134**, 240 (2013).
[4] J. Bandara, H. Weerasinghe, Sol Energy Mater Sol Cell **85**(3), 385 (2005).
[5] Zhang, Yidong, Metal Organic, and Nano-Metal Chemistry **46**(10), 1565 (2016).
[6] M. Jlassi, I. Sta, M. Hajji, H. Ezzaouia, Mater Sci. Semicond. Process **21**, 7 (2014).
[7] R. S. Kate, S. A. Khalate, R. J. Deokate, J. Anal. Appl. Pyrol. **125**, 289 (2017).
[8] N. P. Klochko, K. S. Klepikova, D. O. Zhadan, S. I. Petrushenko, V. R. Kopach, G. S. Khrypunov, V. M. Lyubov, S. V. Dukarov, V. O. Nikitin, M. O. Maslak, A. Yu. Zakovorotniy, A. L. Khrypunova, Mater. Sci. Semicond. Process. **83**, 42 (2018).
[9] S. Nandy, U. N. Maiti, C. K. Ghosh, K. K. Chattopadhyay, J. Phys. Condens. Matter **21**, 115804 (2009).
[10] R. C. Boutwell, M. Wei, A. Scheurer, J. W. Mares, W. V. Schoenfeld, Thin Solid Films **520**, 430212).
[11] S. C Ranjit, R. J. Bulakhe, Optical and Quantum Electronics **51**, 319 (2019).
[12] N. Sadayappan, R. Kwang-Sun, Devices Scientific Reports **9**, 4864 (2019).
[13] J. Zheng, L. Hu, J. S. Yun, M. Zhang, C. F. Lau, J. Bing, A. W. Ho-Baillie, ACS Applied Energy Materials **1**(2), 561 (2018).
[14] M. O. Dawood, S. S. Chiad, A. J. Ghazai, N. F. Habubi, O. M. Abdulmunem, AIP Conference Proceedings **2213**, 020102(2020).
[15] Sh. Kh. Muhammad, E. S. Hassan, K. Y. Qader, Kh. H. Abass, S. S. Chiad, N. F. Habubi, Nano Bio med Eng **12**(1), 67 (2020).
[16] S. S. Chiad, H. A. Noor, O. M. Abdulmunem, N. F. Habubi, IOP Conf. Series: Journal of Physics: Conf. Series **1362**, 012115 (2019).

[17] R. Sharma, A. D. Acharya, S. B. Shrivastava, M. Patidar, M. Gangrade, T. Shripathi, V. Ganesan, Optik Int. J. Light Electron Opt. **127**, 4661 (2016).
[18] J. Tian, H. Deng, L. Sun, H. Kong, P. Yang, and J. Chu, Thin Solid Films **520**(16), 5179(2012).
[19] N. N. Jandow, M. S. Othman, N. F. Habubi1, S. S. Chiad, Kh. A. Mishjil, I. A. Al-Baidhany, Materials Research Express **11**, (2019).
[20] M. M. Hussein, INAE Lett **2**, 35 (2017).
[21] F. N. C. Anyaegbunam, C. Augustine, Digest Journal of Nanomaterials and Biostructures 13(3), 847 (2018).
[22] A. A. Khadayeir, E. S. Hassan, S. S. Chiad, N. F. Habubi, K. H. Abass, M. H. Rahid, T. H Mubarak, M. O. Dawod, I. A. Al-Baidhany, Journal of Physics: Conference Series **1234**(1), 012014 (2019).
[23] A. S. Alkelaby, K. H. Abass, T. H. Mubarak, N. F. Habubi, S. S. Chiad, I. Al-Baidhany, Journal of Global Pharma Technology **11**(4), 347 (2019).
[24] N. N. Jandow, N. F. Habubi, S. S. Chiad, I. A. Al-Baidhany, M. A. Qaeed, International Journal of Nanoelectronics and Materials **12**(1), 1 (2019).
[25] S. S. Chiad, K. H. Abass, T. H. Mubarak, N. F. Habubi, M. K. Mohammed, A. A. Khadayeir, Journal of Global Pharma Technology **11**(4), 369 (019).
[26] M. Kumar, S. Singh, P. K. Tiwari, S. H. Park, Digest Journal of Nanomaterials and Biostructures 15(1), 75 (2020).
[27] A. Echresh, Z. M. Shoushtari, M. Farbod, Appl. Phys. A **119**, 1013 (2015).
[28] S. Sze, K. K. Ng, Physics of Semiconductor Devices, Third Edition (2006).
[29] R. S. Ali, Kh. S. Sharba, A. M. Jabbar, S. S. Chiad, Kh. H. Abass, N. F. Habubi, Journal of NeuroQuantology**18**(1), 26 (2020).
[30] I. A. Elsayed, M. Cavas, R. Gupta, T. Fahmy, A. A. Al-Ghamdi, F. Yakuphanoglu, Journal of Alloys and Compounds **638**, 166 (2015).
[31] M. Cavas, Indian J Phys **92**, 1467 (2018).
[32] I. M. Ibrahima, S. Mohammed, A. Ramizy, Journal of Ovonic Research **14**(1), 17 (2018).
[33] S. Karatas, H. M. El-Nasser, A. Al-Ghamdi, F. Yakuphanoglu, Silicon **10**, 651 (2018).